ELSEVIER

Journal of Photochemistry and Photobiology A: Chemistry 121 (1999) 149–155

Journal of Photochemistry and Photobiology A:Chemistry

Solvent parameter based on the exciplex emission of (2-naphthoxy)polyoxalkyl *p*-cyanobenzoates

Masahide Yasuda[a,*], Yasumasa Kawahito[b], Kiwamu Sasano[b], Yoshito Andou[b], Tsutomu Shiragami[c], Kensuke Shima[b]

[a] *Cooperative Research Center, Miyazaki University, Gakuen-Kibanadai, Miyazaki 889-2192, Japan*
[b] *Department of Materials Science, Faculty of Engineering, Miyazaki University, Gakuen-Kibanadai, Miyazaki 889-2192, Japan*
[c] *Institute for Fundamental Research of Organic Chemistry, Kyushu University, Hakozaki, Higashi-ku, Fukuoka 812-8581, Japan*

Received 14 August 1998; received in revised form 9 November 1998; accepted 15 December 1998

Abstract

The fluorescence spectra of (2-naphthoxy)polyoxalkyl *p*-cyanobenzoates (**1–3**) were analyzed in terms of emission maxima, lifetimes, and quantum yields of the emissions from the locally excited state and the exciplexes (EX) state in 15 kinds of solvents from cyclohexane to acetonitrile. The emission in benzene, toluene, and 1,4-dioxane were deviated from usual Mataga–Lippert plots of EX-emission maxima of **1–3** versus solvent parameter, Δf. In order to modify Δf parameter, we develop new empirical solvent parameter ($E_M(2)$) based on the intramolecular EX emission of 5-(2-naphthoxy)-3-oxa-1-pentyl *p*-cyanobenzoate (**2**). © 1999 Elsevier Science S.A. All rights reserved.

Keywords: Solvent effect; Empirical solvent parameter; Intramolecular exciplex; Mataga–Lippert plots; Naphthoxypolyoxalkyl *p*-cyanobenzoates

1. Introduction

Solvent effect is one of the most fundamental method to analyze the reaction intermediates [1]. Photochemically, the most widely applied solvent effect is Mataga–Lippert (M–L) plots of emission maxima of exciplex (EX) versus the solvent polarity parameter, Δf, which is a function of dielectric constant (ε) and refractive index (n) of the solvent (see Eq. (1)). The M–L plots elucidate the physical properties of EX such as dipole moment (μ) [2,3]. However, many EX emissions are affected not only by the polarity of solvents but also by other properties of solvents such as hydrogen bond, π-electrons, and lone pair electron [4], thus resulting in the scattered M–L plots. Especially, benzene, toluene, and 1,4-dioxane have caused large deviation from M–L plots in many cases [5]. Therefore, the use of these solvents have been avoided in M–L plots in spite of the appearance of EX emission in these solvents. Although an empirical parameter $E_T(30)$ which is based on the absorption spectra of pyridinium *N*-phenoxide betain dye [1] has been a useful scale for solvent polarity, μ can not be derived from the plots versus $E_T(30)$. Therefore, we are interested in the modification of Δf to empirical parameter based on EX emission.

$$\Delta f = \frac{\varepsilon - 1}{2\varepsilon + 1} - \frac{n^2 - 1}{4n^2 + 2} \quad (1)$$

It is essential to observe intense EX emissions in wide range of solvents from non-polar to polar solvents. However, many EX systems, in general, do not show the EX emission in non-polar solvents and very polar solvents because of poor stabilization energy of EX and the dissociation of EX into ion radicals, respectively [6]. Linkage of an electron-donor moiety with an electron-acceptor moiety is effective to observe an intense EX emission [7–9]. Recently we reported that EX emissions from (9-phenanthroxy)alkyl *p*-cyanobenzoate were observed in solvents from benzene to dichloromethane [10]. Here, we develop the empirical solvent parameter based on the intramolecular EX emission of (2-naphthoxy)polyoxalkyl *p*-cyanobenzoate (**1–3**, see Scheme 1) which appeared in solvents from cyclohexane to acetonitrile.

2. Experimental details

2.1. Instruments

^1H and ^{13}C nuclear magnetic resonance (NMR) spectra were taken in $CDCl_3$ on a Bruker AC 250P spectrometer at

*Corresponding author. Tel.: +81-985-58-4785; fax: +81-985-58-3899; e-mail: r00001u@cc.miyazaki-u.ac.jp

1010-6030/99/$ – see front matter
PII: S1010-6030(98)00468-7

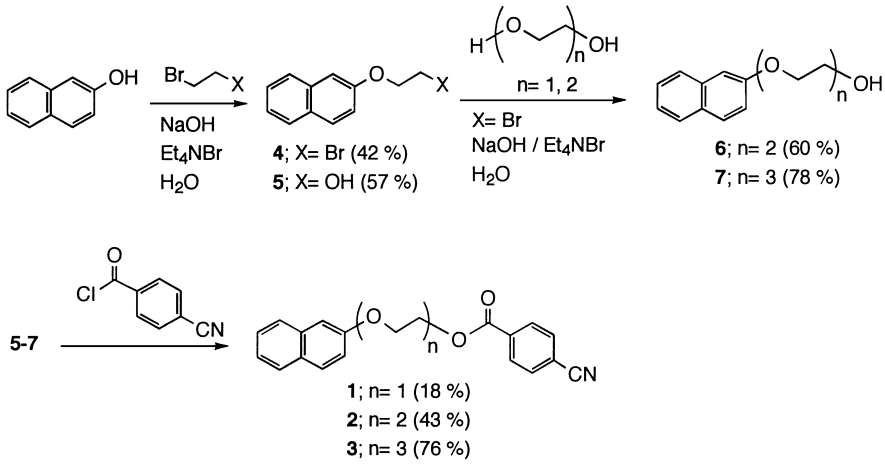

Scheme 1.

250 and 62.9 MHz, respectively. High resolution mass spectra (HRMS) were obtained at an ionizing voltage of 70 eV on a Hitachi M2000A spectrometer. UV spectra were measured on a Hitachi U2001 spectrometer. Oxidation and reduction potentials were measured by the cyclic voltammetry of an acetonitrile solution of **1–3** (1×10^{-2} M) in the presence of a supporting electrolyte; Et_4NBF_4 (0.1 M) at 23°C on a Hokuto Denko HA-501G potentiostat and a HB-105 function generator using a platinum disk working electrode, a carbon counter electrode, and an $Ag/AgNO_3$ reference electrode.

Steady-state fluorescence spectra were measured on a Hitachi F4500 spectrometer. The fluorescence lifetimes were measured by single-photon-counting method on a Horiba NAES 550 spectrometer. For the fluorescence measurement, the concentrations of the solution of **1–3** were adjusted for absorbance to be less than 0.08. After bubbling with argon gas, the fluorescence spectra were observed by excitation at 310 nm. According to the reported method [11], quantum yields for the fluorescence were determined at room temperature using a benzene solution of naphthalene (the quantum yield is 0.19) as an actinometer [12].

2.2. Materials

Spectral grade of cyclohexane, benzene, toluene, and dichloromethane were used without the further purification. 1,4-Dioxane, dibutyl ether, diethyl ether, diisopropyl ether, 1,2-diethoxyethane, tetrahydrofuran, and 1,2-dimethoxyethane were distilled from Na before use. Acetonitrile was distilled from P_2O_5 and then CaH_2. Ethyl acetate, 2-methyl-2-propanol, and 2-propanol were distilled.

2-Naphthol, tetraethylammonium bromide (Et_4NBr), 1,2-dibromoethane, 2-bromoethanol, ethylene glycol, diethylene glycol, and *p*-cyanobenzoyl chloride were obtained from Tokyo Kasei.

2.3. Synthesis of **1–3**

To an aqueous solution (100 ml) containing 2-naphthol (0.1 mol), NaOH (0.1 mol) and Et_4NBr (5 mmol), 1,2-dibromoethane (0.2 mol) was added under stirring at room temperature and refluxed for 3 h. After the reaction mixture was extracted with $CHCl_3$ and washed with water, the crude products were purified by column chromatography on silica gel (BW-300, Fuji Silicia) to give 2-(2-naphthoxy)ethyl bromide (**4**) (Scheme 1). In a similar manner, the reaction of 2-naphthol (0.1 mol) with 2-bromoethanol (0.2 mol) gave 2-(2-naphthoxy)ethanol (**5**). 5-(2-Naphthoxy)-3-oxa-1-pentanol (**6**) and 8-(2-naphthoxy)-3,6-dioxa-1-octanol (**7**) were prepared by refluxing an aqueous solution of **4** (10 mmol) in the presence of Et_4NBr (1 mmol) and NaOH (10 mmol) for 4–5 h with ethylene glycol (50 ml) and diethylene glycol (57 ml), respectively. The preparations of **1–3** were performed by stirring **5–7** (2 mmol) with *p*-cyanobenzoyl chloride (20 mmol) in pyridine (10 ml) at room temperature for 15 h. After the evaporation of pyridine under reduced pressure, the reaction mixture was solved in 150 ml of $CHCl_3$. The $CHCl_3$ solution was washed with dilute HCl aqueous solution to remove residual pyridine and then washed with saturated $NaHCO_3$ solution to remove *p*-cyanobenzoic acid which was produced by hydrolysis of *p*-cyanobenzoyl chloride. The purification of **1–3** was performed by column chromatography on silica gel and repeated recrystallization from ethanol in the cases of **1** and **2**. The spectral data are shown as follows:

2-(2-Naphthoxy)ethyl *p*-cyanobenzoate (**1**): Melting point (m.p.) 111–112°C (from MeOH). ^1H $\delta = 4.44$ (2H, t, $J = 4.4$ Hz), 4.77 (2H, t, $J = 4.4$ Hz), 7.16–7.48 (5H, m), 7.70–7.79 (4H, m), 8.14 (2H, d, $J = 8.3$ Hz); ^{13}C NMR $\delta = 64.13$, 65.74, 106.93, 116.52, 117.91, 118.70, 123.94, 126.54, 126.71, 127.65, 129.16, 129.63, 130.22, 132.19, 133.63, 134.34, 156.34, 164.89. HRMS Calc. for $C_{20}H_{15}NO_3$: 317.0994. Found: 317.1051.

5-(2-Naphthoxy)-3-oxa-1-pentyl *p*-cyanobenzoate (**2**): m.p. 67.0–67.5°C (from MeOH). ^{1}H NMR $\delta = 3.87$–4.03 (4H, m), 4.24 (2H, t, $J = 4.7$ Hz), 4.52 (2H, t, $J = 4.7$ Hz), 7.12 (1H, s), 7.29–7.44 (2H, m), 7.55–7.75 (6H, m), 8.06 (2H, d, $J = 8.3$ Hz); ^{13}C NMR $\delta = 63.59$, 66.30, 67.83, 68.43, 105.56, 114.95, 116.81, 117.73, 122.62, 125.32, 125.61, 126.46, 127.73, 128.21, 128.93, 131.01, 132.62, 133.26, 155.49, 163.58; HRMS Calc. for $C_{22}H_{19}NO_4$: 361.1299. Found: 361.1312.

8-(2-Naphthoxy)-3,6-dioxa-1-octyl *p*-cyanobenzoate (**3**): Oil; ^{1}H NMR $\delta = 3.72$–3.93 (8H, m), 4.22 (2H, t, $J = 4.7$ Hz), 4.50 (2H, t, $J = 4.7$ Hz), 7.10–7.45 (5H, m), 7.62–7.76 (4H, m), 8.09 (2H, d, $J = 8.4$ Hz); ^{13}C NMR $\delta = 64.67$, 67.24, 68.91, 69.95, 70.58, 70.75, 106.53, 116.18, 117.83, 118.78, 123.59, 126.28, 126.59, 127.51, 128.86, 129.27, 129.99, 132.00, 133.70, 134.30, 156,53, 164.77; HRMS Calc. for $C_{24}H_{23}NO_5$: 405.1530. Found: 405.1574.

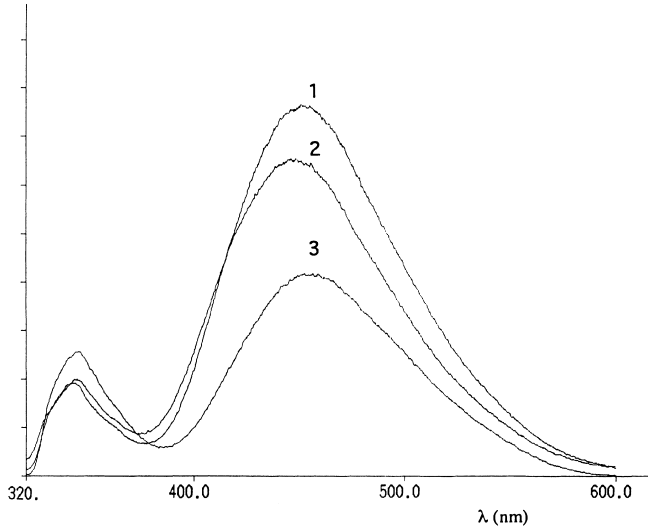

Fig. 1. Fluorescence spectra of **1–3** in diethyl ether: Excitation 310 nm.

3. Results

Fluorescence spectra were measured in typical 15 kinds of solvents. Table 1 lists the solvents used in the present investigation and their Δf parameters. The fluorescence spectra of **1–3** showed an intense emission at a range from 400 to 510 nm dependently on solvent polarity and an emission near 340 nm independently on solvent polarity. The latter emission near 340 nm was similar to that of 2-methoxynaphthalene (**8**), revealing that the emission came from the locally excited state (LE) of 2-naphthoxy group (D) moiety of **1–3**. The former emission at 400–510 nm can be attributed to the emission from the intramolecular exciplex (EX) formed between D and *p*-cyanobenzoate group (A) moieties. Thus, the linkage of D with A by methylene bridge is effective to observe EX emission in wide range of solvent polarity, since the fluorescence of **8** was quenched efficiently by *p*-cyanobenzoate (e.g. propyl *p*-cyanobenzoate) but EX emissions were very weak or were not observed in these solvents. As a typical example, the fluorescence spectra of **1–3** in DE are shown in Fig. 1. The EX emissions of **2** were observed in all 15 kinds of solvents but the EX emissions in PA and AN for **1** and in AN for **3** were not observed. The EX emission maxima (ν_{ex} in cm^{-1}) of **1–3** were summarized in Table 1. The lifetimes (τ_{LE} and τ_{EX}) and the quantum yields (Φ_{LE} and Φ_{EX}) for the fluorescences from LE and EX measured in these solvents are summarized in Table 2.

Table 1
Solvent parameters, fluorescence lifetime of **8**, and emission maxima of **1–3** in various solvents

Solvent[a]	Δf[b]	τ_M^c (ns)	ν_{ex} (10^4 cm^{-1})[d]			$E_M(2)$[e]
			1	**2**	**3**	
CH	0.101	15	2.44	2.45	2.31	0.105
BZ	0.117	13	2.20	2.22	2.17	0.248
DO	0.122	13	2.16	2.19	2.16	0.267
TL	0.127	13	2.23	2.24	2.20	0.236
BE	0.192	14	2.26	2.29	2.24	0.205
PE	0.237	13	2.23	2.26	2.22	0.223
DE	0.256	11	2.22	2.24	2.21	0.236
EE	0.270	13	2.10	2.15	2.11	0.292
EA	0.292	13	2.15	2.16	2.12	0.285
TF	0.309	14	2.11	2.14	2.08	0.298
ME	0.309	13	2.04	2.11	2.06	0.316
DM	0.326	6	2.06	2.09	2.05	0.329
TB	0.347	13	2.04	2.08	1.98	0.335
IP	0.370	13	no[f]	2.02	1.97	0.360
AN	0.393	14	no[f]	1.96	no[f]	0.409

[a] CH – cyclohexane; BZ – benzene; DO – 1,4-dioxane; TL – toluene; BE – dibutyl ether; PE – diisopropyl ether; DE – diethyl ether; EE – 1,2-diethoxyethane; EA – ethyl acetate; TF – tetrahydrofuran; ME – 1,2-dimethoxyethane; DM – dichloromethane; TB – 2-methyl-2-pronanol; IP – 2-pronanol; AN – acetonitrile.
[b] Solvent polarity – $\Delta f = (\varepsilon - 1)/(2\varepsilon + 1) - (n^2 - 1)/(4n^2 + 2)$.
[c] Lifetime of fluorescence of 2-methoxynaphthalene (**8**).
[d] Exciplex emission maxima in cm^{-1}.
[e] New empirical solvent parameter.
[f] Not observed.

4. Discussion

4.1. Exciplex formation

The energy of EX (E_{ex}) is related to Δf by Mataga–Lippert (M–L) (Eq. (2)) where I_p is the ionization potential of D, E_a represents the electron affinity of A, C is the Coulombic interaction energy between the cation radical of D and the anion radical of A, μ is the dipole moment of EX, and ρ represents the effective radius of the solvent cavity [2,3]. Summations of the half-peak of oxidation potential of D (E^{ox}) and the half-peak of the reduction potential of A (E^{red}) were used instead of the summations of I_p and E_a. Since Franck–Condon ground state may be

Table 2
Lifetime and quantum yield for fluorescence of **2** in various solvents

Solvent	τ_{LE}[a] (ns)	(Φ_{LE})[b]	τ_{EX}[a] (ns)	(Φ_{EX})[b]	k_{ex}^{c} (10^8 s^{-1})	k_{f}^{d} (10^6 s^{-1})	k_{d}^{e} (10^7 s^{-1})	$k_{f}^{ex\ f}$ (10^6 s^{-1})	$k_{d}^{ex\ g}$ (10^8 s^{-1})
CH	1.8	(0.005)	11.0	(0.028)	4.9	2.8	6.4	2.9	0.9
BZ	1.1	(0.006)	20.5	(0.025)	8.3	5.0	7.2	1.3	0.5
DO	1.4	(0.013)	22.4	(0.029)	6.4	9.3	6.7	1.4	0.4
TL	2.0	(0.010)	24.9	(0.029)	4.2	5.0	7.2	1.4	0.4
BE	4.1	(0.007)	18.9	(0.027)	1.7	1.6	7.0	2.0	0.5
PE	1.6	(0.007)	16.0	(0.033)	5.4	4.4	7.3	2.4	0.6
DE	2.1	(0.004)	20.0	(0.024)	3.9	1.9	8.9	1.5	0.5
EE	1.2	(0.008)	11.1	(0.008)	7.5	6.6	7.0	0.8	0.9
EA	1.8	(0.006)	8.7	(0.009)	4.8	3.3	7.4	1.2	1.1
TF	0.5	(0.006)	6.6	(0.004)	19.3	12.0	5.8	0.6	1.5
ME	1.2	(0.008)	9.0	(0.005)	7.5	6.5	7.0	0.6	1.1
DM	0.6	(0.005)	9.9	(0.006)	14.9	8.3	17.0	0.6	1.1
TB	1.0	(0.010)	4.2	(0.002)	9.2	10.0	6.9	0.5	2.4
IP	0.7	(0.007)	5.2	(0.001)	13.5	10.0	6.7	0.1	1.9
AN	1.3	(0.005)	7.1	(0.0002)	7.1	4.1	6.7	0.03	1.4

[a] Fluorescence lifetimes of LE state and of EX state.
[b] Quantum yield in LE state and EX state.
[c] Rate constant for the formation of the EX.
[d] Rate constant for the radiative decay from LE state.
[e] Rate constant for non-radiative decay from LE state.
[f] Rate constant for the radiative decay from EX state.
[g] The rate constnats for the non-radiative decay from EX.

destabilized by the solvation energy (E_{sol}) (Eq. (3)), ν_{ex} is related to μ and solvent parameter Δf by Eq. (4) where h is the Planck's constant and c is velocity of light. According to Eq. (4), the intercept (a) in the M–L plot of ν_{ex} versus Δf equals to $(E^{ox} - E^{red} + C)/(hc)$, thus giving the calculated C value. The slope (b) equals to $-2\,\mu^2/(hc\rho^3)$.

Fig. 2 shows the M–L plots of ν_{ex} versus Δf. In the cases of **1** and **2**, the M–L plots gave good linear correlations except for the values in BZ, DO and TL which deviated into shorter wave number from the straight lines. Deviation of ν_{ex} in BZ, TL and DO are due to the interaction of EX with π-electrons or lone pair electron of these solvents. In the case of **3**, the M–L plots except for the values in BZ, DO, and TL consisted of two linear lines with a break at $\Delta f = 0.25$, suggesting that C-T contributions are much lower in the less poplar solvents than $\Delta f = 0.25$. Thus, BZ, TL and DO were 'out-of-line solvents'. Terms a, b and coefficient factor (γ) calculated by least-squares method except for the data of BZ, TL and DO in the M–L plots of Fig. 2 are summarized in Table 3.

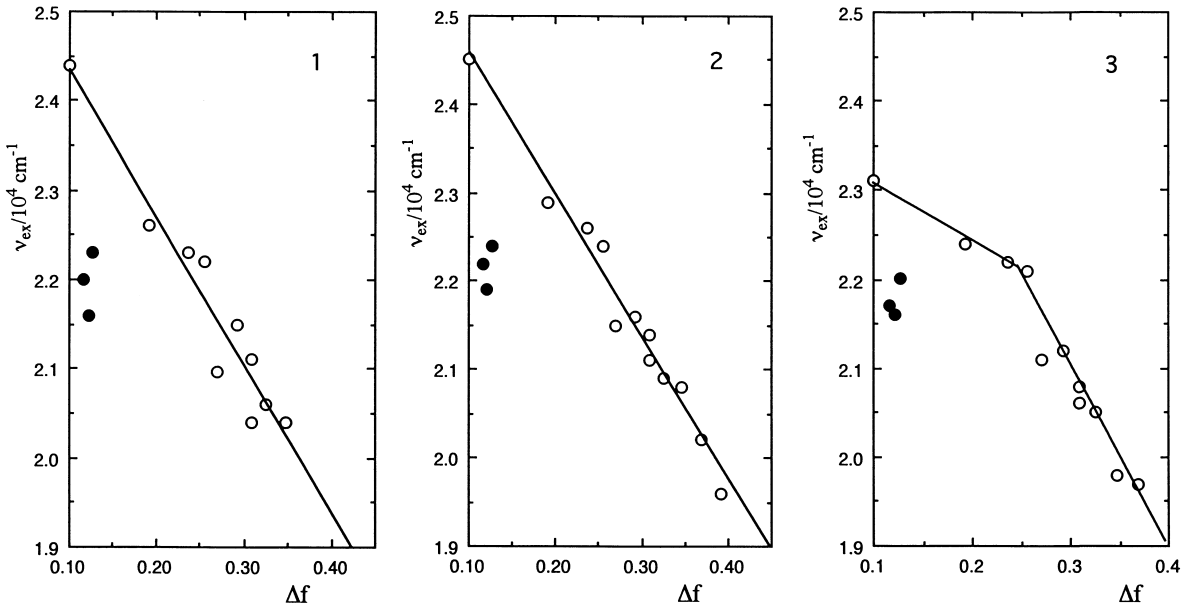

Fig. 2. Mataga–Lippert plots of EX emission maxima (in cm^{-1}) versus Δf in **1–3**: The values (●) in BZ, TL and DO deviated from the straight line.

Table 3
Parameters for the EX state of **1–3**[a]

	1	**2**	**3**[b]
a (10^3 cm^{-1})[c]	26.0	26.2	26.8
b (10^3 cm^{-1})[c]	−16.5	−16.1	−19.6
γ[c]	0.927	0.974	0.911
E^{ox} (V)[d]	1.12	1.01	1.00
E^{red} (V)[e]	−1.98	−1.95	−1.90
$E^{ox} - E^{red}$ (kcal/mol)	71.5	67.6	66.9
C (kcal/mol)[f]	−2.6	−7.0	−9.7
μ (D)[g]	14.1	14.2	15.6
μ (D)[h]	14.3	–	15.5

[a] $E_{O-O} = 83.4$ kcal mol^{-1} (=343 nm).
[b] In the case of **3**, the values of a, b and μ were calculated from the plots in the region of Δf and $E_M(2) > 0.25$.
[c] Terms a, b and γ are the intercept, the slope and the coefficient factor, respectively, for M–L plots of ν_{ex} versus Δf except for the data in BZ, TL, and DO (see Fig. 2).
[d] Half-peak of oxidation potential.
[e] Half-peak of reduction potential.
[f] Coulombic interaction between the cation radical of D and the anion radical of A calculated by Eq. (4).
[g] Dipole moments were calculated from the slopes of Fig. 2 using $\rho = 5$ Å.
[h] Dipole moments were calculated from the slopes of Fig. 4 using $\rho = 5$ Å.

Since ν_{ex} values of **1–3** took similar values irrespective of the length of the bridge, it is suggested that EX takes a sandwich-type structure with usual $\rho = 5$ Å [10,13]. On the basis of this assumption, μ are calculated to be 14.1 and 14.2 D, for **1** and **2**, respectively. Similarly μ of **3** in $\Delta f > 0.25$ is calculated to be 15.6 D.

$$E_{ex} = I_p - E_a - C - \frac{\mu^2}{\rho^3\,\Delta f} \quad (2)$$

$$I_p - E_a = E^{ox} - E^{red}$$

$$h\nu_{ex} = E_{ex} - E_{sol} \quad (3)$$

$$E_{sol} = \frac{\mu^2}{\rho^3\,\Delta f}$$

$$\nu_{ex} = a - b\,\Delta f \quad (4)$$

$$a = \frac{E^{ox} - E^{red} - C}{hc}, \qquad b = \frac{2\mu^2}{hc\rho^3}$$

4.2. Empirical solvent parameter

We selected **2** as a standard molecule to develop new empirical parameters, since **2** showed EX emissions in all 15 kinds of solvents and gave a linear M–L plots with the highest coefficient factor (r) among **1–3** (Table 3).

At first, we estimated the rate constants for EX formation of **2** involving radiative and non-radiative decays from the LE and EX states (Scheme 2). For kinetic analysis, **8** was used as a model compound for analyzing the LE state without the interaction with A. The lifetimes (τ_{LE}) of LE states of **2** were much smaller than the fluorescence lifetimes (τ_M) of **8** which were measured to be 13–15 ns independently on solvent polarity except for DM ($\tau_M = 6$ ns) as shown in Table 1. Therefore, the rate constants (k_{ex}) for the exciplex formation between D and A can be calculated using τ_{LE} and τ_M according to Eq. (5)[14].

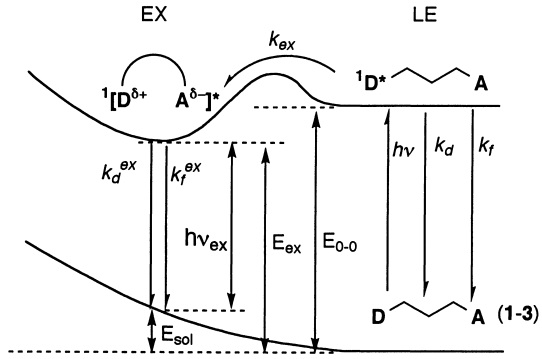

Scheme 2.

$$\tau_{LE}^{-1} = \tau_M^{-1} + k_{ex} \quad (5)$$

$$\Phi_{LE} = \frac{k_f}{k_f + k_d + k_{ex}} = k_f\tau_{LE} \quad (6)$$

$$k_f = \frac{\Phi_{LE}}{\tau_{LE}} \quad (7)$$

$$k_d = \tau_M^{-1} - k_f \quad (8)$$

$$\Phi_{EX} = \frac{k_f^{ex}}{(k_f^{ex} + k_d^{ex})}\frac{k_{ex}}{(k_f + k_d + k_{ex})} = k_f^{ex}k_{ex}\tau_{LE}\tau_{EX} \quad (9)$$

$$k_f^{ex} = \frac{\Phi_{EX}}{k_{ex}\tau_{LE}\tau_{EX}} \quad (10)$$

$$k_d^{ex} = \tau_{EX}^{-1} - k_f^{ex} \quad (11)$$

The fluorescence quantum yield (Φ_{LE}) from LE state is expressed by Eq. (6) where k_f and k_d are the rate constants for the radiative and the non-radiative decay from LE state, respectively. Therefore, k_f and k_d were calculated by Eqs. (7)

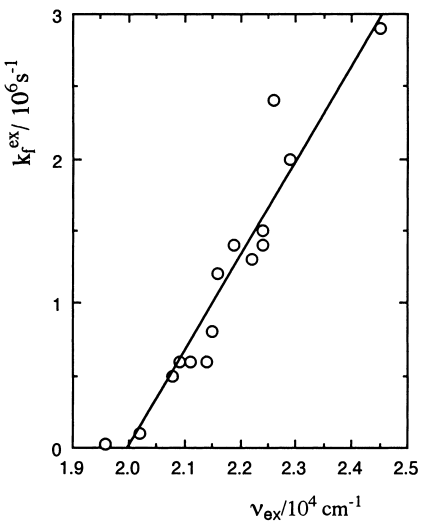

Fig. 3. Plots of k_f^{ex} versus ν_{ex} in **2**.

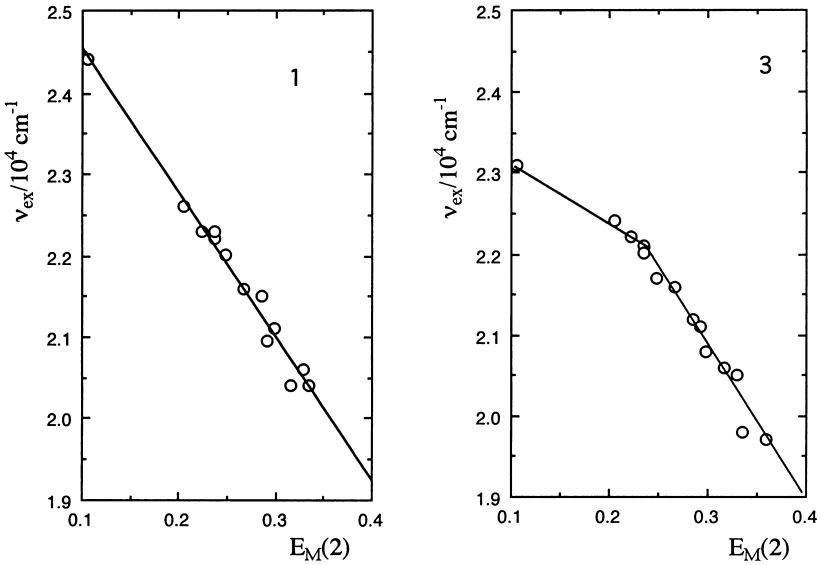

Fig. 4. Mataga–Lippert plots of EX emission maxima versus $E_M(2)$ for (A) **1** and (B) **3**: Coefficient factors were 0.978 for **1** and 0.943 for **3**.

and (8), respectively. Similarly, the quantum yield (Φ_{EX}) of the fluorescence from EX state is represented by Eq. (9). The rate constants for the radiative (k_f^{ex}) and the non-radiative decays (k_d^{ex}) from the EX state were calculated by Eqs. (10) and (11). The calculated rate constants are summarized in Table 2.

The k_d of **2** were nearly constant (5.8–8.9 $\times$ 10^7 s^{-1}) in all solvents except for DM which has a heavy atom effect. Also k_d^{ex} of **2** were nearly constant (0.4 – 1.9 $\times$ 10^8 s^{-1}) in solvents except for TB. On the other hand, the k_f^{ex} gradually decreased as solvent polarity increased. The plots of k_f^{ex} versus ν_{EX} exhibit a smooth decrease in k_f^{ex} with decreasing ν_{EX}, as shown in Fig. 3. The k_f^{ex} appears not to depend upon any specific structural feature [15].

Using **2** as a standard molecule, we modified Δf to empirical solvent-parameter, that we call $E_M(2)$. According to Eq. (12) which is derived from Eq. (4), the $E_M(2)$ values are calculated for 15 kinds of solvents including BZ, TL, and DO using the observed ν_{ex} for **2**, $a = 2.62 \times 10^4$ cm^{-1} and $b = -1.61 \times 10^4$ cm^{-1}. Table 1 lists $E_M(2)$.

$$E_M(2) = \frac{\nu_{ex} - a}{b} \tag{12}$$

$$\nu_{ex} = a - bE_M(2)$$

$$a = \frac{E^{ox} - E^{red} - C}{hc}, \qquad b = \frac{2\mu^2}{hc\rho^3} \tag{13}$$

Fig. 4 shows the M–L plots of ν_{ex} versus $E_M(2)$ for **1** and **3** which showed good linear relationships for all 15 solvents.

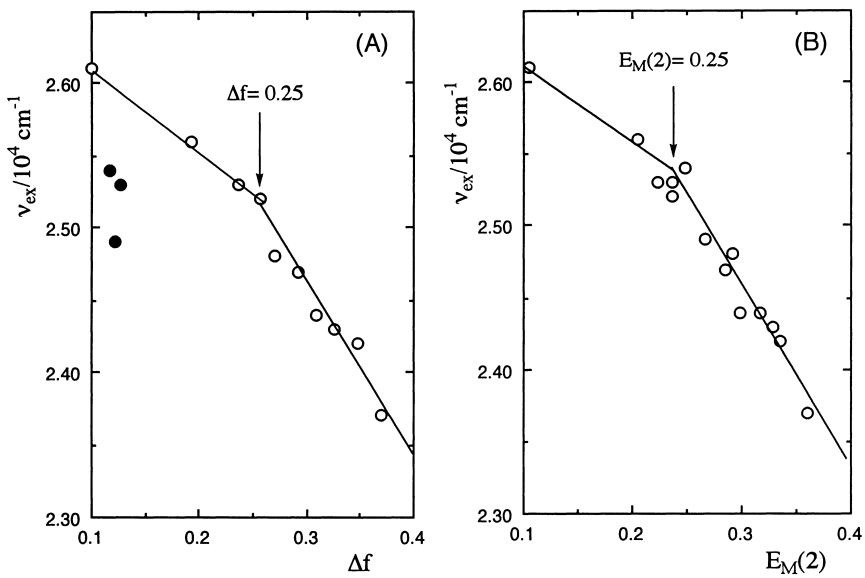

Fig. 5. Mataga–Lippert plots of EX emission maxima versus (A) Δf and (B) $E_M(2)$ for the exciplex between 1-naphthonitrile and ethyl phenyl ether.

The slope can be related to μ according to Eq. (13). Thus, the μ obtained from the M–L plots versus $E_M(2)$ is in good agreement with those from the M–L plots versus Δf (Table 3). These results clearly demonstrate that $E_M(2)$ values can be used instead of Δf values for M–L plots.

We previously reported an intermolecular EX between 1-naphthonitrile (CNN) and ethyl phenyl ether (PhOEt) [5]. Charge-transfer contribution of EX was changed between less-polar and polar solvents, since M–L plots of ν_{ex} versus Δf gave two linear lines with a break at $\Delta f = 0.25$ (Fig. 5). Again, BZ, TL, and DO were out-of-line solvents in this case. Therefore, the M–L plots versus $E_M(2)$ was applied to CNN-PhOEt system. The M–L plots versus $E_M(2)$ gave two linear lines without the deviation in BZ, TL and DO, showing clearly a break point at $E_M(2) = 0.25$ (Fig. 5). Thus, $E_M(2)$ can be applied to the M–L plots in intermolecular EX.

References

[1] C. Reichardt, Solvent Effects in Organic Chemistry, Verlag Chemie, Weiheim, 1978.
[2] N. Mataga, Y. Kaifu, M. Koizumi, Bull. Chem. Soc. Jpn. 28 (1955) 690.
[3] E. Lippert, Z. Naturforch 109 (1955) 541.
[4] Y. Masaki, Y. Uehara, S. Yanagida, C. Pac, J. Chem. Soc., Perkin Trans. 2 (1991) 191.
[5] C. Pac, M. Yasuda, K. Shima, H. Sakurai, Bull. Chem. Soc. Jpn. 55 (1982) 1605.
[6] N. Mataga, in: M. Gordon, W.R. Ware (Eds.), The Exciplex, Academic Press, New York, 1975, p. 113.
[7] T. Okada, N. Mataga, Bull. Chem. Soc. Jpn. 49 (1976) 2190.
[8] A.M. Swinnen, M. Van der Auweraer, F.C. De Schryver, K. Nakatani, T. Okada, N. Mataga, J. Am. Chem. Soc. 109 (1987) 321.
[9] J. Kawakami, M. Iwamura, J. Nakamura, Chem. Lett. (1992) 1013.
[10] M. Yasuda, G. Kuwamura, K. Shima, J. Photochem. Photobiol. A: Chem. 86 (1995) 127.
[11] J.B. Birks, Photophysics of Aromatic Molecules, Wiley, New York, 1970, Chap. 4.
[12] S.L. Murov, Handbook of Photochemistry, Marcel-Dekker, New York, 1973.
[13] F.D. Lewis, G.D. Reddy, D. Bassani, J. Photochem. Photobiol. A: Chem. 65 (1992) 205.
[14] F.D. Lewis, E.L. Burch, J. Phys. Chem. 100 (1996) 4055.
[15] I.R. Gould, R.H. Young, L.J. Muller, S. Farid, J. Am. Chem. Soc. 116 (1994) 8176.